# Atypical transistor-based chaotic oscillators: Design, realization, and diversity

Ludovico Minati, Mattia Frasca, Paweł Oświęcimka, Luca Faes, and Stanisław Drożdż

## Articles you may be interested in

Constructing an autonomous system with infinitely many chaotic attractors
Chaos: An Interdisciplinary Journal of Nonlinear Science **27**, 071101 (2017); 10.1063/1.4986356

Synchronization of chaotic systems
Chaos: An Interdisciplinary Journal of Nonlinear Science **25**, 097611 (2015); 10.1063/1.4917383

How close are time series to power tail Lévy diffusions?
Chaos: An Interdisciplinary Journal of Nonlinear Science **27**, 073112 (2017); 10.1063/1.4986496

Hidden hyperchaos and electronic circuit application in a 5D self-exciting homopolar disc dynamo
Chaos: An Interdisciplinary Journal of Nonlinear Science **27**, 033101 (2017); 10.1063/1.4977417

Revival of oscillations from deaths in diffusively coupled nonlinear systems: Theory and experiment
Chaos: An Interdisciplinary Journal of Nonlinear Science **27**, 061101 (2017); 10.1063/1.4984927

Information theory and robotics meet to study predator-prey interactions
Chaos: An Interdisciplinary Journal of Nonlinear Science **27**, 073111 (2017); 10.1063/1.4990051

# Atypical transistor-based chaotic oscillators: Design, realization, and diversity

Ludovico Minati,[1,2,a)] Mattia Frasca,[3] Paweł Oświęcimka,[1] Luca Faes,[4,5] and Stanisław Drożdż[1,6]

[1]*Complex Systems Theory Department, Institute of Nuclear Physics Polish Academy of Sciences (IFJ-PAN), Kraków, Poland*
[2]*Centre for Mind/Brain Science (CIMeC), University of Trento, Trento, Italy*
[3]*Department of Electrical Electronic and Computer Engineering (DIEEI), University of Catania, Catania, Italy*
[4]*Healthcare Research and Innovation Program, Foundation Bruno Kessler (FBK), Trento, Italy*
[5]*BIOTech, Department of Industrial Engineering, University of Trento, Trento, Italy*
[6]*Faculty of Physics, Mathematics and Computer Science, Cracow University of Technology, Kraków, Poland*

In this paper, we show that novel autonomous chaotic oscillators based on one or two bipolar junction transistors and a limited number of passive components can be obtained via random search with suitable heuristics. Chaos is a pervasive occurrence in these circuits, particularly after manual adjustment of a variable resistor placed in series with the supply voltage source. Following this approach, 49 unique circuits generating chaotic signals when physically realized were designed, representing the largest collection of circuits of this kind to date. These circuits are atypical as they do not trivially map onto known topologies or variations thereof. They feature diverse spectra and predominantly anti-persistent monofractal dynamics. Notably, we recurrently found a circuit comprising one resistor, one transistor, two inductors, and one capacitor, which generates a range of attractors depending on the parameter values. We also found a circuit yielding an irregular quantized spike-train resembling some aspects of neural discharge and another one generating a double-scroll attractor, which represent the smallest known transistor-based embodiments of these behaviors. Through three representative examples, we additionally show that diffusive coupling of heterogeneous oscillators of this kind may give rise to complex entrainment, such as lag synchronization with directed information transfer and generalized synchronization. The replicability and reproducibility of the experimental findings are good. *Published by AIP Publishing.*
[http://dx.doi.org/10.1063/1.4994815]

**Transistor-based oscillators have been a ubiquitous staple of electronics for decades, generating periodic signals in disparate applications, e.g., communications, timing, and sound generation. It has been established that small circuits comprising at most few transistors can also generate chaotic signals, which have complex features and are inherently unpredictable, though not random. Among other reasons, such chaotic oscillators have attracted interest for their ability to replicate some phenomena occurring in biological systems when interconnected in networks. However, to date surprisingly little is known about how to obtain them, even whether they represent "unusual" or "special" situations. Here, a large number of transistor-based chaotic oscillators were automatically designed. These circuits do not trivially represent known topologies, or variations thereof, and are therefore "atypical." They were physically built, then studied in terms of their overall features and certain cases of particular interest. Despite their simplicity, they generated a diverse range of signals and behaviors, including some typically associated with other systems.**

**The circuit diagrams and signals from all of them are provided, considerably expanding the available repertoire of oscillators of this kind.**

## I. INTRODUCTION

Countless low-order continuous-time systems exhibit chaos for certain combinations of parameter values; new examples are continuously identified,[1] including recent advances in systems with lines of equilibria,[2,3] hidden attractors,[4,5] and memristors.[6,7] While the underlying nonlinearities often involve polynomial terms or products of the state variables, many functions are suitable for obtaining chaos.[8] Mathematical models can be transformed into analog circuits following a consolidated approach[9,10] wherein each state variable is associated with a physical circuit quantity (e.g., voltage across a capacitor or current through an inductor), and the nonlinearity is realized exploiting the characteristics of a semiconductor device or approximated by piecewise linear functions. Efforts towards discovering or designing simple chaotic systems and implementing them physically are significant.[11] To the circuits obtained following this approach, one should add many others which generate

---
a)Author to whom correspondence should be addressed: lminati@ieee.org, ludovico.minati@unitn.it, and ludovico.minati@ifj.edu.pl. Tel.: +39 335 486 670. URL: http://www.lminati.it.

chaotic dynamics by design such as the well-known Chua's circuit,[12–17] and those which can exhibit chaos as an undesired or unexpected feature (e.g., power converters[18] and oscillators[19]). Chaotic circuits feature nonlinearities originating from diverse devices including diodes, varactors,[20] operational amplifiers,[21] ferroelectric components,[22] and memristors.[23]

Compared to the general abundance of known chaotic oscillators, relatively few circuit topologies based on a small number of discrete bipolar junction-transistors (BJTs), including non-autonomous[24,25] and autonomous[26–30] circuits, have been reported to date. Discrete BJTs have served as the fundamental staple of electronics for decades, and an extensive repertoire of circuits has been developed to serve signal generation, amplification, and processing functions, for example, in radio and audio applications. Hence, this paucity is surprising. Indeed, although there exist methodologies or, at least, guidelines to design chaotic circuits based, for instance, on the interaction of active networks and passive nonlinear devices,[14] on time-delay systems,[16] and on operational amplifiers,[31] we are not aware of general techniques yielding circuits based on a limited number of discrete BJTs as the only source of nonlinearity. The instances of such circuits reported in the literature have been arrived at either by serendipity or by following specific considerations: many stem from modifications of existing periodic oscillators (e.g., the Colpitts oscillator,[26] the Hartley oscillator,[27] the blocking oscillator,[28] and the inductor-resistance-diode circuit[24]), or implement particular principles such as disturbance of integration, which underlies the non-autonomous Lindberg–Murali–Tamasevicius (LMT) chaotic circuit.[25]

A preliminary study addressing this issue attempted to use genetic algorithms, wherein evolution was driven towards obtaining high-entropy signals in SPICE simulations, and arbitrary circuit topologies were searched for by representing connections and component values as a bit-string.[32] A number of autonomous chaotic oscillators were successfully obtained, some of which were subsequently characterized experimentally.[30] One of them, featuring particularly small size (1 BJT, 2 inductors and 1 capacitor), was later used as a building block to realize large networks, which were able to replicate some emergent phenomena originally observed in biological neural systems.[33,34] That study, however, had severe limitations. First, it did not address to what extent the evolutionary aspect of the genetic algorithm was significant, compared to the random search component introduced by random cross-over and finite mutation probability. When circuit topology and component values are conjointly represented, the majority of individuals resulting from cross-over are expected to be structurally invalid or inactive oscillators. Second, the individual fitness was determined based on SPICE simulations, whose level of agreement with experimental measurements had not been evaluated; indeed, several studies have indicated that it can be poor for chaotic oscillators of this kind.[30,35,36] The accuracy of such simulations was certainly also constrained by the fact that the circuits were physically realized by means of low-end commercially-available components, associated with significant parasitics and simplified models. The study

introduced, nevertheless, the useful notion of connecting a variable resistor in series to the fixed DC supply voltage powering the circuits, and using it as a control parameter to manually search for chaotic ranges; owing to this, it was possible to obtain chaotic dynamics with diverse properties in the physical realizations of the circuits.[32]

Here, we report on a multitude of chaotic oscillators based on a limited number of passive components alongside one or two BJTs as the only source of nonlinearity. These circuits were obtained by means of a random search over the space of $2^{85}$ possibilities according to a bit-string representing discrete component values, in terms of a catalog of commercially-available devices, and the connections between them. Heuristic rules were applied to substantially reduce the search space by excluding invalid individuals. One hundred circuits were chosen based on SPICE simulations, physically realized with state-of-the-art components, and experimentally characterized. We illustrate their overall characteristics with a focus on some cases of particular interest. In addition to expanding the available repertoire of oscillator circuits of this kind, this work posits that there is nothing "special" or "unusual" about BJT-based chaotic oscillators; on the contrary, chaoticity is a common occurrence in valid BJT-based oscillator circuits.

## II. OSCILLATOR DESIGN AND REALIZATION

### A. Search and simulation

Similar to Ref. 32, each oscillator was encoded as a random string of 85 bits, allocated as shown in Fig. 1(a) to represent a circuit with up to 8 nodes (including 5 V DC supply via resistor, and ground), 1 supply series resistor (value $R$, 16 value steps in $R = 464 \ldots 2150 \, \Omega$), 6 inductors or capacitors (1 bit determining type, value $L$ or $C$, 8 values of each in $C = 150 \ldots 1000 \, \text{pF}$ and $L = 15 \ldots 220 \, \mu\text{H}$), and 2 BJTs of fixed NPN type. The circuit was represented as a graph and iteratively pruned until convergence, eliminating those elements that (i) had multiple terminals connected to the same node (i.e., short-circuited components), or (ii) did not have paths to both ground and supply nodes either directly or via other elements, or (iii) had terminals not connected to at least another component. Moreover, if (i) the circuit contained fewer than two elements with connections to the ground and supply nodes, or (ii) there was a path between the supply and ground nodes comprising inductors only, or (iii) the supply series resistor had been eliminated, the pruning process was also canceled, and the individual discarded. If the process completed and the circuit contained at least 1 inductor, 1 capacitor, and 1 BJT, the circuit was considered "valid" and the corresponding SPICE netlist was written; otherwise it was rejected as "invalid." With the exception of not allowing BJTs connected as diodes, effectively these rules did not alter the outcome of the random search, only accelerating the process by eliminating outright individuals that could not oscillate in SPICE simulation. Similar search approaches have been applied to other areas of electronic circuit design, including layout optimization.[37,38]

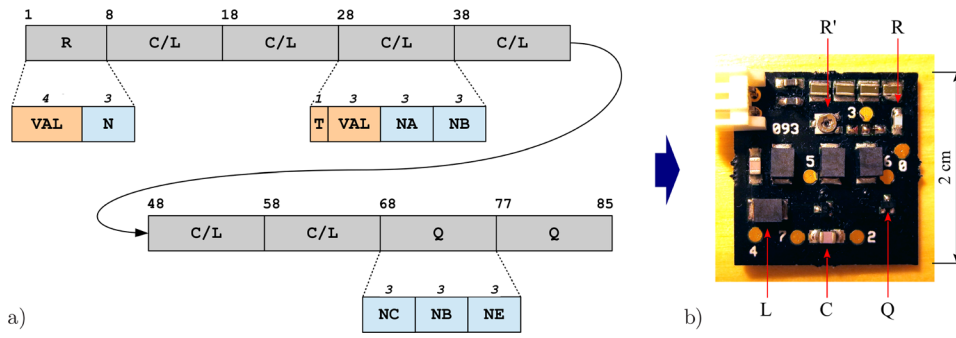An initial SPICE simulation was performed for each valid circuit, running to 200 $\mu$s with a maximum step of

FIG. 1. Circuit encoding and physical realization. (a) Bit-string representing, in order, the DC supply voltage series resistor (R; value VAL and connection node N), six capacitors or inductors (C/L; type T, value VAL and connection nodes NA, NB), and two bipolar-junction transistors (Q; connection nodes NC, NB, NE). (b) Circuit board, comprising selectable fixed (*R*) or variable series resistor (trimmer, *R′*), alongside capacitors (*C*), inductors (*L*), transistors (*Q*), and node probing points (0–7).

10 ns, ramping up the supply voltage during 100 μs, and maintaining default `trtol` and `reltol` settings. The time-series segments for $t > 175$ μs were detrended with a 3rd-degree polynomial, and oscillations were deemed present if resulting peak-to-peak voltage values ranged >100 mV. Circuits with at last one node meeting such a criterion were deemed "active," the others were rejected as "inactive." A second SPICE simulation was performed for each active circuit, running to 1 ms with a maximum step of 1 ns and reducing `reltol` to 0.0001.

The time-series for $t > 500$ μs were linearly interpolated to produce a fixed sampling time-series with a sampling interval of 1 ns. The "dominant period" was found based on the cross-correlation function, and the data were windowed and resampled to yield 10 000 points within 50 times this interval. The resulting time-series were cut into 4 segments of 2500 points, and if the peak-to-peak voltage value was >100 mV, the correlation dimension $D_2$ was calculated for each segment, using the Grassberger-Procaccia method implemented as in Ref. 39, applying non-linear noise reduction with an embedding dimension $\tau/2$, and setting time-delay embedding $\tau$ to the first minimum of the lag mutual information function, embedding dimension $m$ to the minimum value yielding <5% false nearest neighbors, and Theiler window $w$ to twice the first maximum of the space-time separation plot.

The search was performed on a Cray XD1 system (Cray Inc., Seattle WA, USA) running `ngspice-26`.[40] Out of $\approx 2 \times 10^6$ hypothetical oscillators considered (corresponding to an extremely small fraction of all possible ones), $\approx 1.5 \times 10^6$ (i.e., the vast majority) were invalid, and $\approx 4 \times 10^5$ were inactive. Only $\approx 2500$ were active and unique, out of which, in the longer simulations, $\approx 250$ were found not to sustain oscillation and thus discarded. In these simulations, the series resistor value had to be encoded and treated like other parameters rather than being continuously swept, as this would have resulted in an intractable computational load.

### B. Construction and measurement

Among the individuals classified as unique and active, the 100 circuits having the largest $D_2$ across all nodes in simulation ($1.7 \pm 0.7$, median ± inter-quartile range) were physically realized on custom-designed printed-circuit boards, which also comprised a variable resistor to allow searching *a posteriori* for chaotic ranges, and an LC power-supply

decoupling filter [Fig. 1(b)]. The commercially-available components utilized for circuit realization, listed in Supplementary Table I, were chosen attempting to maximize simulation accuracy, namely, (i) inductors were shielded and provided with realistic RLC models, which were necessary as non-ideal behaviour and self-resonance could contribute additional dynamical complexity with respect to a circuit built with ideal inductors,[41] (ii) capacitors had high Q and were optimized for RF operation, and (iii) NPN BJTs (type PRF949; NXP Semiconductor, Eindhoven, The Netherlands) had a transition frequency in the GHz range, limiting the effect of junction capacitances for oscillation in the low MHz range. The circuits were realized verbatim, without simplifying trivial serial or parallel combinations. All board fabrication files are provided as the supplementary material.

Each circuit was measured twice at each node, once powered via the fixed series resistor of the prescribed value (*R*), once via the variable one adjusted manually (*R′*) attempting to obtain chaoticity as in Refs. 30 and 32. As detailed in Subsection III B, the latter set of measurements were primarily considered, as the manual resistor adjustment enhanced the probability of observing chaos. Measurements were performed using low-capacitance probes (model AP020, connected to WavePro 940 oscilloscope; LeCroy Inc., Chestnut Ridge, NY, USA) in AC-coupled differential configuration with respect to local ground to minimize circuit disturbance, yielding 434 time-series of 250 000 points at 500 MSa/s, of which 35 were disregarded due to signal peak-to-peak amplitude <100 mV or issues with correlation dimension estimation; one circuit (no. 40) did not oscillate. All raw time-series are freely available.[42]

The correlation dimension was thereafter calculated as described above for each time-series cut in 10 segments of 25 000 pts. each; the median correlation dimension ($D_2$), its estimation error ($\delta D_2$, spread of curves within identified scaling range, representing level of self-similarity), and variability across segments ($\Delta D_2$, inter-quartile range of $D_2$, representing level of stationarity) were recorded. Non-linear noise reduction was applied to reduce quantization effects; analogous results were obtained with low-pass filtering (data not shown).

## III. RESULTS

### A. Overall features

As shown in Fig. 2(a), clustering applying the DBSCAN algorithm[43] to [$D_2$, $\delta D_2$, $\Delta D_2$] given settings $\varepsilon = 0.2$ and
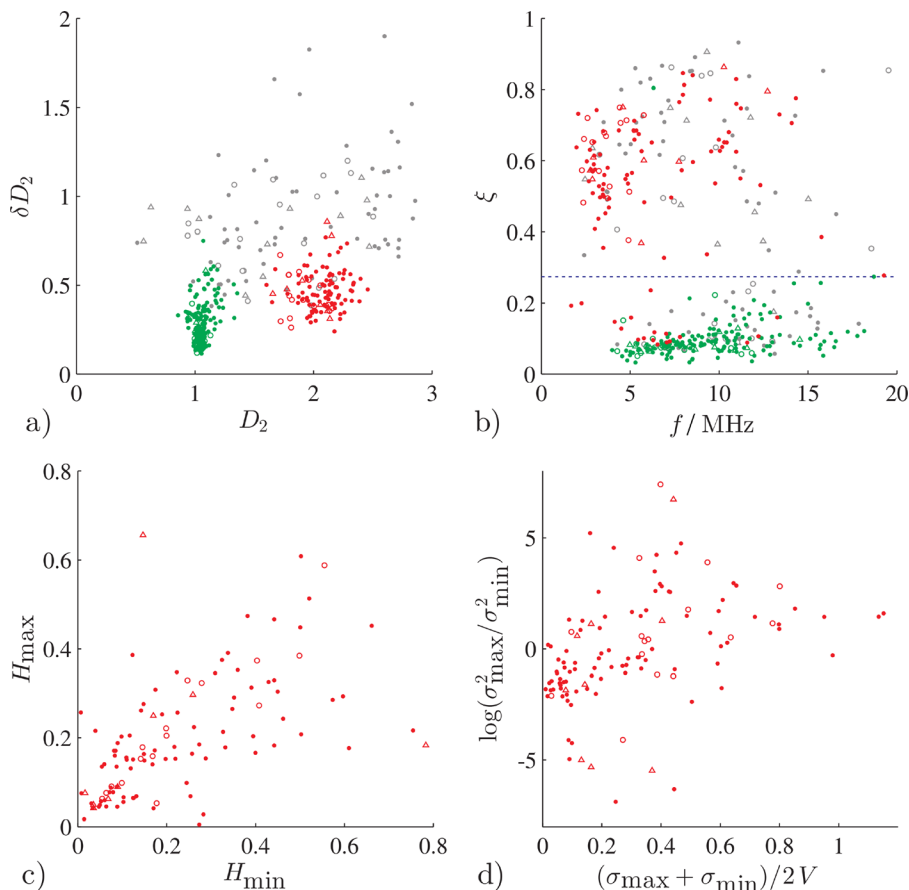
FIG. 2. Signal parameters from the 100 realized oscillators (one point per node, multiple nodes per oscillator). (a) Correlation dimension ($D_2$) and its uncertainty ($\delta D_2$), revealing two clusters corresponding to periodic (green) and chaotic (red) dynamics (gray: unclassified). (b) Spectral centroid ($f$) and flatness ($\xi$), indicating broader spectra at lower frequencies for the chaotic signals. (c) Hurst exponents of maxima and minima amplitudes, indicating correlation and predominant anti-persistent behavior ($H < 1/2$). (d) Amplitude variance asymmetry and average standard deviation, denoting fluctuations of diverse amplitude with sine-like, positive-, and negative-spiking features. Triangles, hollow, and filled circles: circuits with 4, 5, and more components in addition to the resistor.

$\mathrm{min_{pts}} = 20$ automatically identified two clusters, corresponding to periodic ($n = 178$, $D_2 = 1.05 \pm 0.06$) and chaotic ($n = 117$, $D_2 = 2.10 \pm 0.21$) signals, alongside a smaller number of unclassified signals ($n = 104$, e.g., due to poor convergence of the correlation dimension curves in the chosen sampling window, or intermittency). As shown in Fig. 2(b), the chaotic signals had a lower spectral centroid[44] ($f = 5.10 \pm 4.68$ vs. $9.05 \pm 4.16$ MHz), reflecting greater generation of slow fluctuations and, correspondingly, markedly higher amplitude spectral flatness[45] ($\xi = 0.57 \pm 0.20$ vs. $0.08 \pm 0.03$, considered range 5%–95% for $f < 10$ MHz). Assuming as boundary the maximum flatness observed in periodic signals after rejection of one outlier, $\xi < 0.27$, 18 signals misclassified by DBSCAN as chaotic were found to be actually quasi-periodic, and accordingly had a comb-like spectrum.[46] The characteristics of all signals are detailed in supplementary material Table II. Altogether, these experimental results confirm that it is possible to obtain novel BJT-based chaotic oscillators of diverse circuit topology and features, based on a simple random search with suitable heuristics.

Multifractal detrended fluctuation analysis (MFDFA) over $q = -4 \ldots 4$ with a detrending order $m = 2$ was subsequently performed to determine the singularity spectrum $f(\alpha)$ on the chaotic time-series, extracting separately minima and maxima to query the structure of amplitude fluctuations.[47–49] There were 30 signals for which the width $\Delta\alpha > 0.2$ of $f(\alpha)$ suggests potential multifractality, but this was rejected in all cases by consideration of the reshuffled and phase-randomized time-series (also for larger range of $q$, data not

shown).[50] This result indicates that even though chaoticity was pervasive, the circuits did not produce multifractal dynamics. Due to limited time-series length (median 1200 pts., analysis omitted if $<500$ pts.) and need for manual adjustment of pick-picking procedure given widely heterogeneous signal features, this analysis should be considered tentative. Consideration of the Hurst exponent[48,49,51] [shown in Fig. 2(c)] for $q = 2$ revealed an anti-persistent monofractal behavior as a pervasive feature of these circuits ($H_{\max} < 1/2$ for 90% and $H_{\min} < 1/2$ for 84% of signals, where $H_{\max}$ and $H_{\min}$ denote, respectively, the Hurst exponent of the time-series of maxima and minima, rank correlation between them $r = 0.68$), plausibly following energy storage in the capacitor(s). Furthermore, consideration of amplitude variance asymmetry [Fig. 2(d)] indicated that, in agreement with previous observations,[30] these circuits generated signals with diverse sine-like and positive/negative spike-like features ($\log(\sigma_{max}^2/\sigma_{min}^2) = -0.4 \pm 3.0$). To the authors' knowledge, this is the first attempt to query the mono- or multifractal nature of dynamics in BJT-based circuits of the present kind, even though multifractality has been reported for a more complex circuit with stochastic dynamics.[52]

Circuit features predicting chaoticity were searched for by comparing the subsets of circuits generating chaotic and periodic signals at all nodes (33 vs. 46) based on 52 measures, including counts of components, series, parallel and tapped LC combinations, single- and double-transistor topologies, LC tank frequencies, and their relationships. As no significant association was found, the details are not presented, and the view that chaos generation in these circuits

involves a complex relationship between circuit structure and component values is reinforced.[10] The circuits generating at least one chaotic signal according to DBSCAN (49 in total) comprised 1 (1–4; median, range) capacitor, 3 (2–5) inductors, 2 (1–2) BJTs, 6 (4–8) components excluding the resistor, 5 (4–7) nodes, and 4 (1–8) LC combinations.

The full circuit diagrams of the 49 identified chaotic oscillators, with associated waveforms, spectra, and attractors, are provided as supplementary material.

### B. Simulation and measurement reliability

SPICE simulations had good accuracy predicting signal amplitude (measured as voltage inter-quartile range, $r = 0.75$ and $r' = 0.63$, where $r$ and $r'$ denote, respectively, rank-order correlation between simulation and measurement before and after manual resistor adjustment) and spectral centroid $f$ ($r = 0.71$ and $r' = 0.69$); however, they were poor at predicting chaoticity, as indicated by weak correlation between simulations and experiment for both spectral flatness $\xi$ ($r = 0.14$ and $r' = 0.17$) and correlation dimension $D_2$ ($r = 0.07$ and $r' = 0.17$). This situation is in agreement with previous observations for a chaotic Colpitts oscillator,[35] the LMT circuit,[36] and other "atypical" circuits,[30] but this study is the first to systematically consider the issue of the accuracy of SPICE simulations in a large set of BJT-based chaotic circuits. While detailed investigation of this disagreement is beyond the scope of this work, we performed additional simulations with more stringent tolerance and step settings, and rerun correlation dimension estimates for SPICE waveforms attempting to closely replicate the experimental settings (fixed sample rate, filtering <20 MHz, additive Gaussian noise of 5 mV). No relevant improvement in agreement was observed (data not shown). As discussed below, uncertainties in the component parameters and the loading effect of oscilloscope probe connection plausibly contributed to the disagreement, but are unlikely to be the main cause, because the reliability of experimental measurements was good.

Further DBSCAN analyses indicated that, compared to using the simulated resistor value, manual resistor adjustment ($|R - R'|$ median absolute 679 $\Omega$, relative 53%) yielded chaoticity in an additional $\approx$12% of measured signals. Eventually, $\approx$47% of signals were not chaotic regardless of their status in simulations, $\approx$22% were chaotic according to both, $\approx$10% were chaotic in the realized circuits but not in simulation, and $\approx$22% were not classified. Overall, these findings indicated that (i) regardless of careful experimental choices aiming to maximize agreement with simulations, accurate prediction of chaoticity was not possible and (ii) chaoticity was nevertheless a rather common occurrence in the chosen subset of 100 circuits which simulations identified as "active," particularly when the series resistor was manually adjusted.

To gain further insight into measurement reliability, the 15 circuits generating the signals with highest $D_2$ (yielding 43 signals when considering all their nodes) were re-evaluated. First, measurement repeatability was assessed by re-acquiring data after >6 months: small errors for amplitude

(median absolute 6.3 mV, relative 1.7%), centroid frequency $f$ (43.1 kHz, 0.8%), spectral flatness $\xi$ (0.012, 2.8%), and correlation dimension $D_2$ (0.07, 3.1%) indicated that it was very good. Second, measurement reproducibility was assessed by building a second specimen of each oscillator from different components: errors were larger but still small, for amplitude (25 mV, relative 5.8%), centroid frequency $f$ (244.3 kHz, 3.1%), spectral flatness $\xi$ (0.021, 5.3%), and correlation dimension $D_2$ (0.12, 6.3%), indicating that it was also good. For 8 of these second specimens, as a consequence of component tolerances, series resistor readjustment was necessary to obtain chaoticity ($|\Delta R'|$ median absolute 142 $\Omega$, relative 14.0%). Third, the loading effect of attaching the oscilloscope probe (approximately $C = 3.9$ pF, $R_p = 10^6 \Omega$, $R_s = 150 \Omega$) was assessed by repeating all acquisitions multiple times, each time connecting a third probe to another node, and considering the worst-case deviation. Errors were considerably larger for amplitude (56 mV, relative 13.7%), centroid frequency $f$ (717.0 kHz, 13.5%), spectral flatness $\xi$ (0.111, 39.8%). and correlation dimension $D_2$ (0.22, 10.3%), indicating that, at least for some oscillators, the effect of loading was more important than other error sources. Altogether, these results (summarized in supplementary material Fig. S1) reveal that despite the ±10% tolerance in the capacitor and inductor parameters and ±30% tolerance in BJT parameters such as $h_{FE}$, the reliability of the experimental findings was overall good, conferring practical value to the experimental results on the present extended collection of oscillators.

### C. Smallest-size and other representative circuits

The smallest-size chaotic oscillators, which required 4 components in addition to the resistor, consistently featured the topology shown in Fig. 3(a), which comprised 2 inductors and 1 capacitor. The inductors connected the supply node to the base and collector of the BJT, which rendered the currents through them inter-dependent. Remarkably, in the random search, this circuit topology recurred 7 times with only minimal variations (e.g., BJT orientation) but different values of the inductors and the capacitor (Table I). As a function of such values, upon time-delay embedding of the experimentally measured signals, diverse dynamics were observed, including spiral, phase-coherent attractors [Figs. 3(b), 3(d), and 3(e)], attractors resembling the Rössler funnel attractor [Figs. 3(c) and 3(g)], and attractors associated with a spiking behavior [Figs. 3(f) and 3(h)].[10,46] Both period-doubling and quasi-periodicity (possibly favored by the presence of LC tanks with mismatched frequencies) route-to-chaos were observed in these circuits, a result that is relevant as quasi-periodicity has been previously suggested as the prevalent route-to-chaos mechanism in transistor-based chaotic circuits.[30]

The smallest-size BJT circuit previously studied in Refs. 30 and 32 was not identified, possibly due to the more restricted component value ranges considered here, which excluded its indicated inductor and capacitor values; however, two variations of this circuit, including extra elements, were indeed found [circuits no. 21 and 23, see Figs. 4(b) and 4(c)].
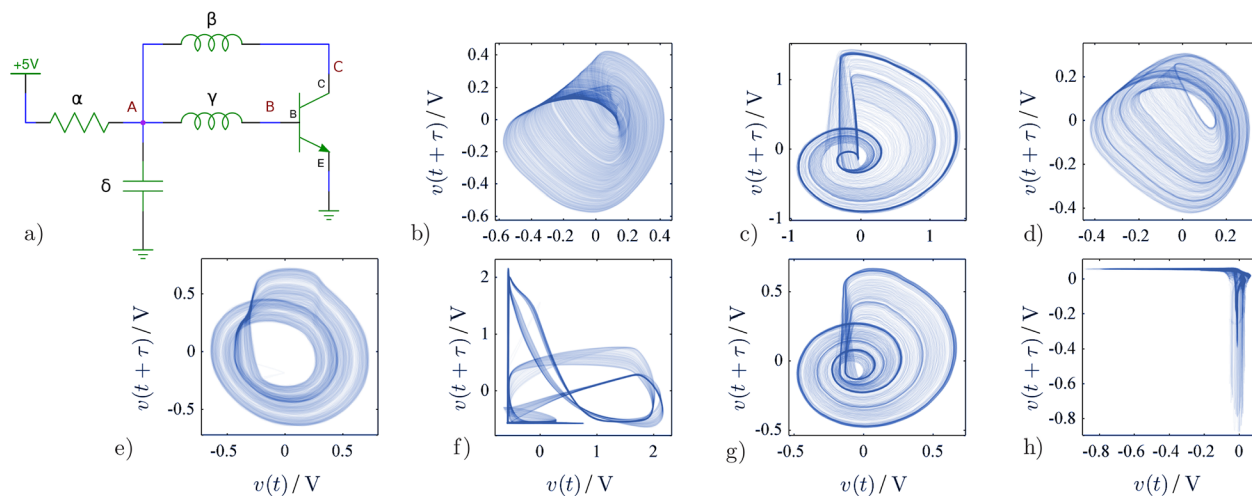
FIG. 3. Smallest chaotic oscillator obtained, and diversity of corresponding attractors. (a) Circuit comprising one resistor (value $\alpha$, where $\alpha = R'$), one BJT, two inductors (values $\beta$, $\gamma$), and one capacitor ($\delta$). (b)–(h) Time-lag attractors obtained for the 7 instances of this circuit with component values as in Table I. The time-lag attractors were reconstructed from signals at node A, except at node C in (f) and node B in (h). For (b), (d), and (f), the BJT was in reverse configuration (i.e., with emitter and collector exchanged). For (e), the resistor was connected to node B instead of A.

Considering the circuits with 5 components in addition to the resistor, 9 occurrences were found, in this case with heterogeneous topology. Two of them [circuits no. 9 and 69; Fig. 4(a) and supplementary material Figs. S2(a) and S2(f)] represented a variation of the smallest-size topology obtained by "degenerating" the supply or ground node by means of an additional inductor. A further one [no. 34; supplementary material Fig. S2(c)] was similar, with the additional inductor providing an extra tap to the supply node. Two others [no. 42 and 90, supplementary Figs. S2(d) and S2(i)] were structurally identical and contained two series inductors; the remaining ones were all different. None represented a straightforward variation of a known circuit topology, and considerable diversity of attractors was again observed.

Further representative examples of the dynamics and diversity observed in the larger circuits are shown in Fig. 4. All spectra were characterized by a dominant component surrounded by a multitude of narrow-band peaks [e.g., Figs. 4(b), 4(c), and 4(f)] and varying intensity of broad-band content [e.g., Figs. 4(a), 4(d), and 4(e)]. Instances of Rössler-like funnel attractors [Figs. 4(a) and 4(f)], attractors similar to the one of the Colpitts oscillator[26] [Fig. 4(c)], reminiscent of Shilnikov chaos[53,54] [Fig. 4(d)], and an attractor with a peculiar triple butterfly like shape [Fig. 4(e)] were observed; instances of quasi-periodicity were also observed [Fig. 4(b)]. In all cases, close overlap in the spectra and attractors from

two different oscillator specimens was observed, confirming good reliability of the experimental results.

### D. Two notable circuits

Two further circuits demonstrated dynamics that were particularly noteworthy. The first one (circuit no. 54), shown in Fig. 5(a), consisted of two cascaded BTJs overlaid to a network of 3 inductors in series and 1 capacitor, which provided multiple feedback paths. While at one node it generated a Rössler-like funnel attractor [Fig. 4(f)], at another node this circuit generated activity resembling a bursting spike-train, with spikes (i.e., impulses of approximately quantized height) appearing as positive fluctuation followed by smaller negative undershoot, having duration $\approx 0.25\,\mu s$ [Fig. 5(b)]. All-or-nothing response was confirmed considering the distribution of local maxima amplitudes ($<25\,MHz$, 3rd-order low-pass filtering, 20 points window, 1 000 000 points at 100 MSa/s, 10 repetitions), which showed clear bimodal distribution with low-amplitude fluctuations in the range of 0–0.5 V and spikes in the range of 2–2.5 V [Fig. 5(c)]; the threshold for spike detection was therefore set to 1 V. The resulting distribution of inter-event intervals (IEI) was discrete, with largest peaks at $\approx 0.9$, 1.9, 2.9 $\mu s$, median $1.9 \pm 1.9\,\mu s$ [Fig. 5(d)]; consideration of signals at other nodes indicated that this discontinuous distribution emerged because the spikes were generated according to underlying oscillation with a relatively strong dominant frequency component [Fig. 4(f)]. The temporal Fano factor $F_t$,[55,56] computed for time windows having a width of $1.3\ldots655.4\,\mu s$, was consistently under-dispersed with respect to a Poissonian distribution ($<1$) at all scales, also with respect to the reshuffled data, and no power-law scaling region was identifiable [Fig. 5(e)]. The distribution $p(s)$ of avalanche size, calculated counting the number of events $s$ in each avalanche and setting the maximum spacing equal to the mean IEI as customary,[55,56] was accordingly exponential-like, showing a substantial overlap between the experimental and reshuffled data [Fig. 5(f)]. A simple auto-regressive

TABLE I. Inductor and capacitor values for the oscillator shown Fig. 3(a).

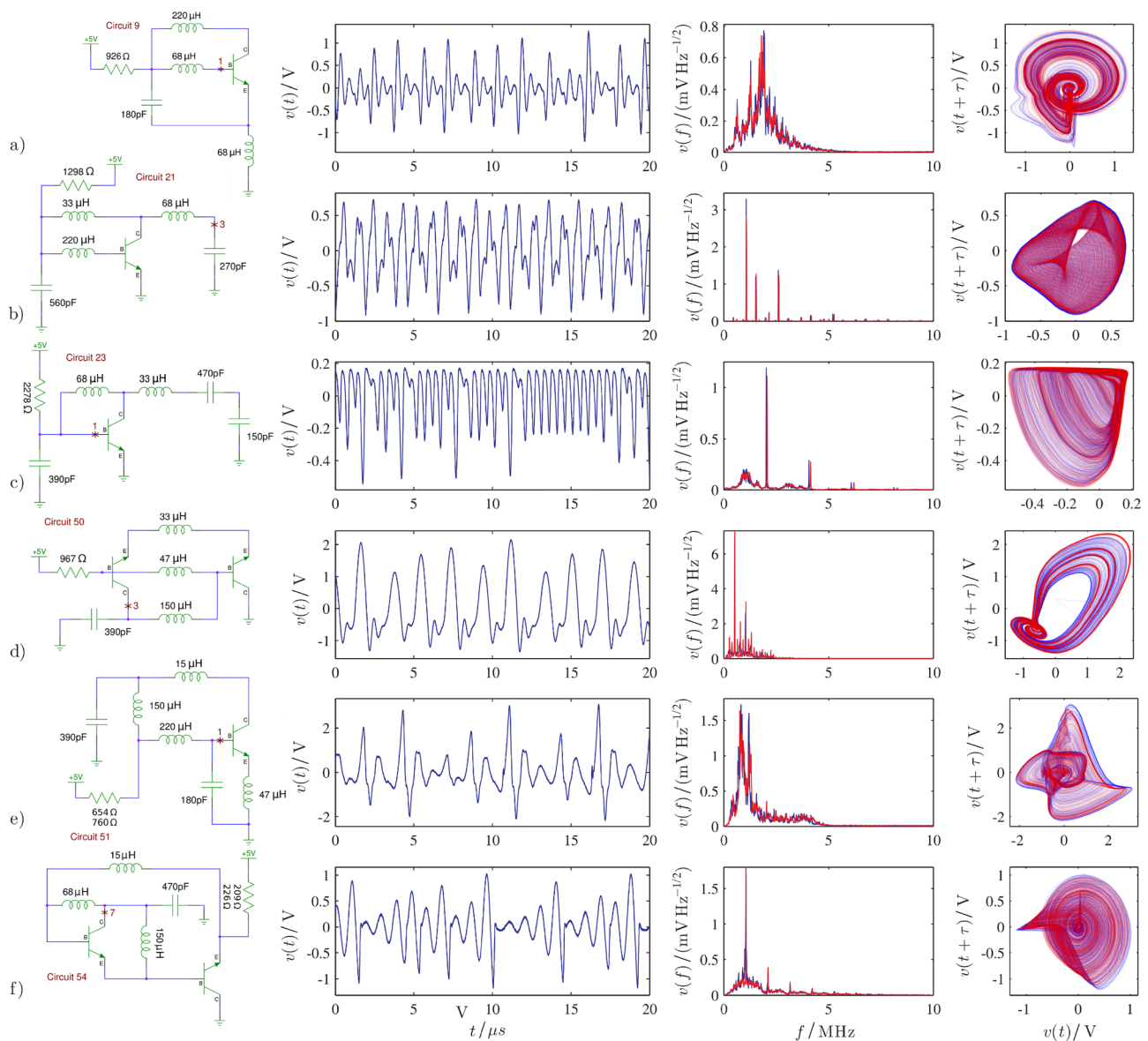| Circuit no. | $\alpha = R'$ ($\Omega$) | $\beta$ ($\mu H$) | $\gamma$ ($\mu H$) | $\delta$ (pF) | Attractor |
|---|---|---|---|---|---|
| 37 | 3460 | 33 | 33 | 150 | Fig. 3(b) |
| 43 | 769 | 150 | 33 | 390 | Fig. 3(c) |
| 49 | 4170 | 100 | 100 | 390 | Fig. 3(d) |
| 53 | 1539 | 220 | 15 | 220 | Fig. 3(e) |
| 67 | 4310 | 150 | 150 | 390 | Fig. 3(f) |
| 70 | 978 | 220 | 15 | 220 | Fig. 3(g) |
| 88 | 1450 | 220 | 47 | 180 | Fig. 3(h) |

FIG. 4. Selection of oscillators having heterogeneous size, temporal, and spectral features: (a) circuit with 5 components, in addition to the resistor; (b), (c), (d), and (f) circuits with 6 components; (e) circuit with 7 components. Replicability was confirmed by a close overlap between measurements from two physical specimens (blue, red; different series resistor values where indicated).

network[57] receiving two consecutive IEIs as input and having 10 hidden neurons could predict the next IEI until $\approx 3\,\mu s$ [rank-order $r > 0.85$, Fig. 5(g), for representative example]. Altogether, these findings indicate that the oscillator has all-or-nothing dynamics which at the surface recall those of neural action potentials:[56] however, even though the spike trains qualitatively resembled bursts (avalanches), the dynamics were not critical and the over-dispersion hallmarking "true" burstiness was not present.[58] Chaotic variants of BJT-based blocking oscillators, which by their nature generate brief pulses, have been proposed for broadband signal generation,[28] and generation of bursts of pulses has been observed;[59] however, to the authors' knowledge, the present circuit does not represent a variation of a known topology. In particular, oscillators generating a quantized response have been previously described,[61] but to the authors' knowledge, this is the first report of an autonomous BJT-based oscillator with this behaviour; quantized spiking and bursting are more

often observed in complex circuits intentionally developed as electronic models of neural dynamics.[60] Future work should explore the possibility of rendering this oscillator critical. Also in this case, there was a good overlap between two specimens realized from different components.

The second circuit (no. 81), shown in Fig. 6(a), consisted of two BJTs with a junction connected in anti-parallel, 2 inductors and 1 capacitor. Separate consideration of the time-series at nodes 3 and 4 indicated that this oscillator combined generation of continuous irregular activity with switching between two unstable foci, resulting in a double-scroll attractor [Figs. 6(b) and 6(c)]. Besides a complex spectrum featuring a large number of resonances overlapped to broad activity [Fig. 6(d)], voltage at node 4 of this circuit revealed a clear asymmetric double-scroll attractor [Fig. 6(e)] which was visible not only with time-delay embedding but also when plotted with respect to voltage at node 3 [Fig. 6(f)]. Also for this oscillator, agreement between two
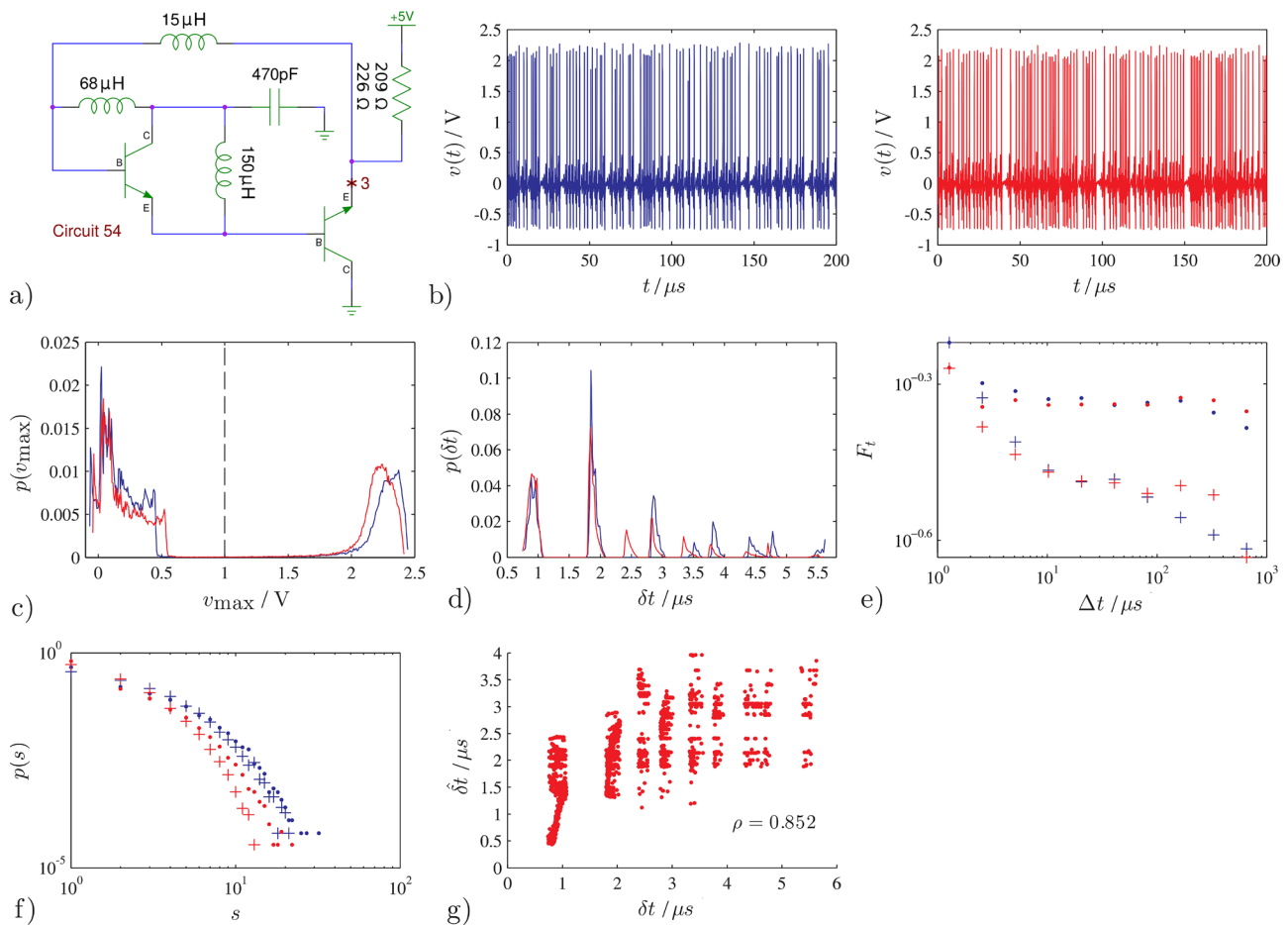
FIG. 5. Spiking chaotic oscillator. (a) Circuit diagram. (b) Time-series recorded at node 3 in two physical specimens (blue, red; different series resistor values), demonstrating replicable generation of spikes and bursts. (c) Distribution of maxima amplitudes $v_{max}$, confirming all-or-nothing behavior (dashed line: spike detection threshold). (d) Distribution of inter-event intervals $\delta t$, revealing discrete steps. (e) Distribution of temporal Fano factor $F_t$ for experimental and reshuffled series (dots, crosses), showing under-dispersion and absence of a power-law scaling region. (f) Corresponding distribution $p(s)$ of avalanche size $s$, showing absence of heavy tail. (g) Scatter-plot between predicted $\hat{\delta t}$ and measured $\delta t$ (nonlinear auto-regression) inter-event intervals for representative time-series, wherein strong correlation confirms deterministic dynamics.

realized specimens was good. The double-scroll attractor is characteristic of Chua's circuit, a paradigmatic circuit that has been realized in many distinct ways, including operational amplifier-based nonlinearities, inductor-less implementations, cellular neural network layouts, and monolithic designs; these implementations start from the system equations and subsequently implement the characteristic function of the Chua's diode in several ways, or reinterpret the state variables to obtain an equivalent circuit.[9] Here, the circuit was not been intentionally designed to produce a double-scroll chaotic attractor, but rather was obtained by serendipity. To the authors' knowledge, it is the simplest known BJT-based circuit producing a double-scroll attractor. Another embodiment of Chua's circuit only using 2 BJTs as active elements has been previously described; however, it also includes 7 resistors, 2 diodes, 2 capacitors and 1 inductor (total 15 elements).[62] More recently, an inductorless double-scroll chaotic oscillator has been proposed; however, since it is based on the RC phase shift, it also requires a large number of components in addition to the 2 BJTs, namely, 7 resistors and 4 capacitors (total 13 elements).[63] The present circuit requires less than half the number of components (total 6 elements), and as such is particularly important

towards proving the generative potential of small BJT-based oscillators.

## E. Synchronization

While the synchronization of structurally different chaotic systems has been thoroughly studied, experimental data on heterogeneous BJT-based oscillators are limited.[64] Here, three paradigmatic cases are shown based on arbitrarily chosen circuit pairs, to demonstrate the capability of these circuits to yield complex synchronization phenomena when coupled into network configurations.

Three oscillator pairs were physically realized on a dedicated substrate inside a ceramic dual-in-line package, to simultaneously show the potential for integration into a hybrid module usable for realizing large networks. These modules included read-out amplifiers to minimize oscillator loading (type MAX4200; Maxim Inc., San Jose, CA, USA). A dedicated test board was developed, including additional current adjustment (jointly for the two oscillators) and facilities for hardware-based generation of bit-streams based on maxima amplitudes for use as entropy sources; while this feature was not utilized for the present study, its full design
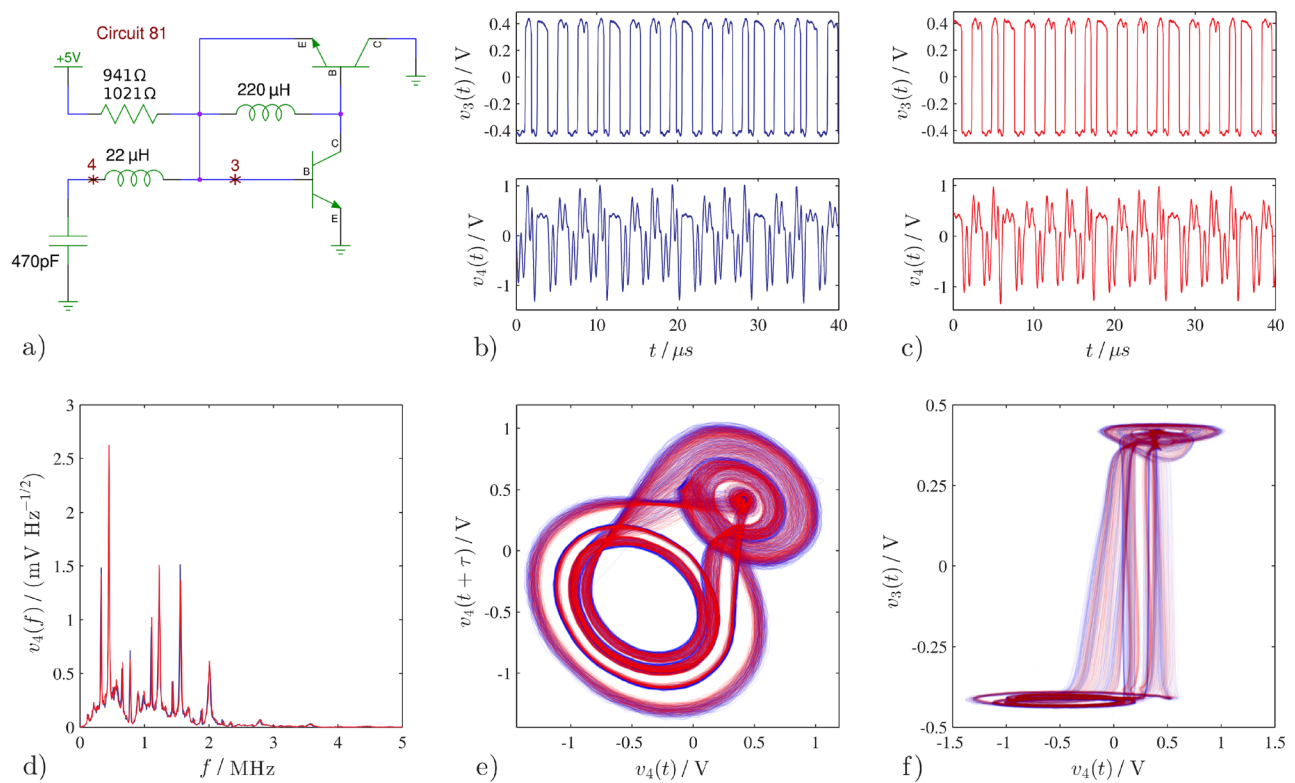
FIG. 6. Double-scroll chaotic oscillator. (a) Circuit diagram. (b) and (c) Time-series recorded from two physical specimens (blue, red; different series resistor values), showing irregular amplitude fluctuations at node 4 and switching behavior at node 3. (d) Amplitude spectra recorded at node 4, demonstrating replicable generation of multi-component, broad spectrum. (e) Time-lag attractor reconstruction revealing asymmetric double-scroll geometry, closely overlapping between the specimens (recorded with oscilloscope probe attached to node 4 only). (f) Corresponding physical-variable attractor reconstruction in voltages at nodes 3 and 4.

is provided alongside that of the modules as [supplementary material](). In all three cases considered the coupling was diffusive, i.e., implemented by means of a resistor, with an additional DC-blocking capacitor to avoid exchange of biasing current. The coupling nodes, series supply, and coupling resistor values were determined empirically. All raw time-series are freely available.[42]

The first case, shown in Fig. 7(a), demonstrates the emergence of lag synchronization, wherein oscillator $X$ leads $Y$ by $\delta \approx 0.1 \, \mu s$ over a predominant period of $\approx 1.5 \, \mu s$, as shown by time-lag normalized mutual information. To confirm asymmetric information flow, the transfer entropy was estimated on 10 time-series pairs (25 000 pts.) according to the method proposed in Ref. 65, which makes use of the nearest-neighbor entropy estimator[66] (implemented with $k_{neigh} = 10$) and employs a non-uniform embedding technique to limit the dimension of the variables involved in the computation.[67] The transfer entropy was considerably larger in the $X \rightarrow Y$ than in the $Y \rightarrow X$ direction, with $0.264 \pm 0.009$ vs. $0.144 \pm 0.005$, and the self-entropy was comparable between $X$ and $Y$, with $3.10 \pm 0.019$ and $3.27 \pm 0.02$; the corresponding correlation dimension was $D_2 = 2.48 \pm 0.12$ and $2.48 \pm 0.15$, confirming chaoticity. While lag synchronization is a common observation in weakly coupled heterogeneous oscillators,[64] it does not straightforwardly imply asymmetric information flow in the direction of the lag. It has been shown that measures such as delayed mutual information can be misleading in this regard.[68] Here, asymmetric information flow was confirmed

using transfer entropy, which overcomes the problems of possible spurious detected coupling over uncoupled directions often encountered using time-delayed mutual information.[68,69]

The second case, shown in Fig. 7(b), demonstrates the achievement of near-complete synchronization between structurally different oscillators. The phase-coherence value between the time-series for $X$ and $Y$ was $0.95 \pm 0.001$, and the corresponding maximum cross-correlation coefficient of amplitude fluctuations extracted via Hilbert's transform was $0.979 \pm 0.0001$. The corresponding correlation dimension values were $D_2 = 2.53 \pm 0.20$ and $2.51 \pm 0.35$, confirming that near-complete synchronization could be attained without incurring oscillation death or destroying chaoticity. This demonstrates the possibility of obtaining an almost-invariant manifold between the two continuous chaotic systems.[64,70]

The third case, shown in Fig. 7(c), demonstrates the possibility of obtaining generalized synchronization, wherein a complex functional relationship of the form $\mathbf{y}(t) = \psi(\mathbf{x}(t))$ is established, instead of one between the scalar time-series. Induction and detection of generalized synchronization are non-trivial problems, particularly when dealing with experimental systems whose dynamics are often influenced by small parametric variations and parasitics, meaning that analytical approaches are difficult to apply.[64,71,72] We resorted to a metric based on agnostically determining whether closeness in response space implies closeness in driving space: the $L$-index[73] was calculated for 10 time-series pairs (12 500 pts. each), time-delay embedded according to lag $\tau$ set to the
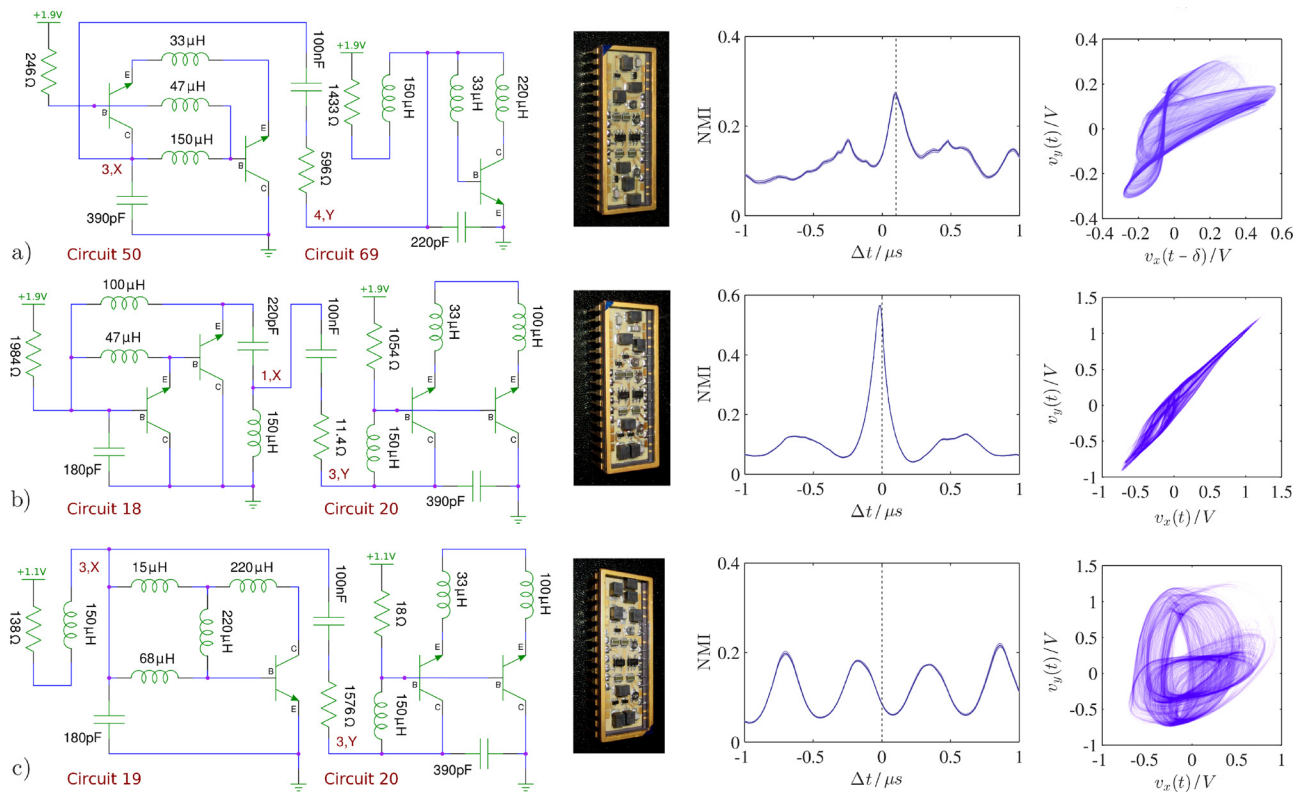
FIG. 7. Examples of coupled heterogeneous oscillators showing, in order, circuit diagram, physical realization, time-lag normalized mutual information plot, and Lissajous figure. Configurations yielding (a) lag synchronization, (b) near-complete synchronization, and (c) generalized synchronization. $v_s < 5$ V due to shared current-adjustment circuitry on test board.

first minimum of mutual information, dimension $m = 1 \dots 4$ and $k_{\text{neigh}} = 10$. The maximum $L$-value between directions was considered, and steadily increased with embedding dimension $m$, reflecting representation of increasingly complex synchronization manifold geometry: synchronization was weak for $m = 1$ ($0.144 \pm 0.006$), substantially increased for $m = 2$ ($0.752 \pm 0.014$), increased further for $m = 3$ ($0.905 \pm 0.002$), and reached a level effectively indicating complete synchronization for $m = 4$ ($0.951 \pm 0.007$). The corresponding correlation dimension values were $D_2 = 2.79 \pm 0.16$ and $2.79 \pm 0.28$, confirming chaoticity. A similar situation was also observed for the circuit in Fig. 7(a). Generalized synchronization has been obtained numerically and experimentally for diverse nonlinear electronic circuits, mostly based on operational amplifiers, unidirectional coupling, or other more complex arrangements.[71,74–77] To the authors' knowledge, this is the first experimental observation in which it spontaneously emerged between two diffusely coupled BJT-based oscillators.

Multifractal detrended fluctuation analysis (MFDFA) was also applied to the time-series of minima and maxima generated by these coupled oscillators under a variety of settings, but no evidence of multifractality was obtained (data not shown).

## IV. CONCLUSIONS

The results presented in this work highlight that chaos is a common occurrence in small electronic circuits wherein the only sources of non-linearity are the $v$–$i$ characteristics in the bipolar junction-transistor(s), and wherein self-sustained oscillation is present. In the circuits considered here, the probability of observing chaos was enhanced through instantiating a variable resistor connected in series to the DC supply voltage, whose resistance represented the main control parameter and was purposefully adjusted searching for chaotic ranges. The observation of chaos in approximately half of the realized circuits (notably preselected among those who featured self-sustained oscillation), despite the limited accuracy of simulations in predicting chaoticity, indicates that chaotic oscillators of this kind are definitely neither "uncommon" nor "special"; considering them as such would only be a consequence of the fact that a formal synthesis method is still missing, and that the limited existing literature focuses on chaotic adaptations of canonical topologies or circuits discovered by serendipity.[24–30]

By contrast, critical phenomena were not detected. Further, the dynamics provided no convincing instances of multifractality; however, anti-persistent mono-fractal dynamics were prevalent. There are thus profound differences with respect to many self-organized biological and physical systems, which often dwell close to the point of criticality and exhibit signatures of multifractality.[48,49,78,79] In particular, criticality in electronic circuits has received very limited attention thus far, but a recent study on a lattice of glow lamps has demonstrated the possibility of eliciting critical phenomena by external tuning, even in the absence of opportunity for self-organization to drive dynamics towards criticality.[55] It should be noted that the target of these simulations and experiments was obtaining chaoticity,

not criticality; hence, the proximity of phase-transition points, where critical phenomena preferentially occur, was not explored systematically.

Owing to the fact that chaos is a pervasive occurrence in these circuits, atypical topologies of chaotic oscillators, previously unknown and not intentionally representing variations of existing ones, could be identified by means of a random search process. The search process was made computationally tractable by applying suitable heuristics, eliminating *a-priori* invalid circuits without attempting to simulate them, and then using a two-step approach to only run time-consuming simulations for circuits already ascertained to be oscillating; this "funnel" approach meant that time-consuming simulations were run only a small fraction of the initial candidates ($\approx 0.1\%$). While the usage of genetic algorithms to design these circuits was previously advocated,[32] the present results suggest that maintaining a similar bit-stream representation of circuit topology and parameters, the search process can effectively be approximated by a random one. Such assertion is supported by the fact that, when crossing-over the genetic code of two different oscillators, the majority of resulting circuits are not functioning oscillators, as observed for other situations where structures and parameters are conjointly represented. Future work may reconsider the use of genetic algorithms applied in a narrower scope for the optimization of parameter values in these circuits.[37,38]

Compared to preexisting work,[30,32] significant instrumental improvements were introduced, attempting to enhance the accuracy of SPICE simulations; in particular, the physical inductors were modeled by means of realistic RLC networks, high-grade capacitors and transistors with low parasitics were chosen, and interconnections were realized with optimized printed circuit boards. Nevertheless, SPICE simulations could only predict with good accuracy the amplitude and frequency centroid of the generated signals, but they were unsuccessful at predicting onset of chaos, as indexed by uncoupled spectral flatness and correlation dimension in comparison to the experimental data. Because the reproducibility of the experimental results across circuit specimens realized with different components was good, such disagreement could not only be due to parametric mismatches between physical components and canonical values. This result thus highlights limitations inherent in the component models and numerical solver. A substantial number of chaotic oscillators were nevertheless identified, owing to the fact that (i) as stated above, chaoticity is a common occurrence in these circuits, (ii) these circuits included a supply series resistor, which was intentionally adjusted searching for chaotic ranges, (iii) even though the simulations failed to predict chaoticity, they successfully delivered a set of atypical circuits all of which (except one) actually oscillated when physically realized: this restricted the search to a very small fraction of the entire set of hypothetical oscillators described by the generated random bit-strings.

A recurrent topology was identified in circuits comprising 4 elements in addition to the series resistor. To the authors' knowledge, it did not represent a previously known oscillator, and it demonstrated a remarkable universality in

that the 7 instances found generated a range of diverse attractors as a function of the component values. The size of this circuit is comparable to the smallest known autonomous oscillators of this kind.[26–28,30] Even though a formal route-to-chaos analysis was not conducted, both period-doubling cascade and quasi-periodicity were commonly observed and identified as primary mechanisms to the onset of chaos in these circuits.

Furthermore, two novel oscillators noteworthy for their dynamics were obtained. The first one generated spikes approximating an all-or-nothing (quantized) response. Analyses of temporal scaling and predictability of inter-event intervals indicated that the underlying dynamics were strongly deterministic, and signatures of criticality such as power-law scaling of avalanche size were missing. Nevertheless, this oscillator is of particular interest, as it demonstrates the possibility of observing chaoticity in transistor-based circuits in the form of irregular inter-event times between spikes, rather than cycle amplitude fluctuations. While a range of quantized oscillators capable of generating spikes and bursts have been described previously, these often implement integrate-and-fire dynamics based either on considerably more complex circuits aiming to mimic neurons[60] or on highly non-linear components such as glow lamps (gas discharge tubes).[55] Even though critical signatures were missing, there were elements of qualitative similarity to neural discharge time-series; hence future work should explore the possibility of modifying or externally tuning this circuit to yield critical behavior.

The second oscillator generated an asymmetric double-scroll attractor via combining irregular cycle amplitude fluctuations and alternation between two unstable foci. There are a variety of numerical and experimental systems, which can give rise to this attractor, of which to the authors' knowledge only two implementations based on bipolar-junction transistors are known.[62,63] Compared to them, the circuit considered in this study is considerably smaller as it involves less than half the total number of elements, namely, 2 inductors, 2 transistors, 1 capacitor, and 1 resistor, and as such, it reinforces the universality of these oscillators.

By means of three arbitrary but representative examples, it was also demonstrated that structurally heterogeneous circuits can be diffusively coupled, giving rise to non-trivial synchronization scenarios. While diffusive (resistive) coupling is inherently symmetrical, it was shown that, depending on the oscillator dynamics, asymmetric inter-dependency can emerge, hallmarked by lag synchronization and directed information transfer between the two oscillators. It was also demonstrated that in some cases an invariant synchronization manifold may exist enabling near-complete synchronization between different oscillators, without incurring in oscillation death or loss of chaos. Furthermore, the possibility of spontaneous emergence of generalized synchronization was shown, by means of applying a rank-based affinity metric, which consistently increased up to four-dimensional embedding. Taken together, these results demonstrate the potential of these circuits to spontaneously generate non-trivial synchronization phenomena, leading to network complexity when coupled in heterogeneous ensembles, as is often the case in natural systems; this is of broad interest since, to date,

limited experimental research has been done on emergence in networks of electronic oscillators mismatched structurally rather than just parametrically.[64,80,81]

More generally, this study provides a large collection of transistor-based chaotic circuits, with substantial diversity of topological and dynamical features. All circuit diagrams and experimental time-series are freely available, supporting future research and applications in this area, particularly as the findings were largely reproducible across realizations of each circuit.

## SUPPLEMENTARY MATERIAL

See supplementary material for additional tables, figures, circuit diagrams, signals, circuit board fabrication materials, and illustrations.

## ACKNOWLEDGMENTS

[1]J. C. Sprott, Int. J. Bifurcation Chaos **21**, 2391 (2011).
[2]S. Jafari and J. C. Sprott, Chaos, Solitons Fractals **57**, 79 (2013).
[3]C. Li, J. C. Sprott, and W. Thio, J. Exp. Theor. Phys. **118**, 494 (2014).
[4]S. Jafari, J. C. Sprott, and F. Nazarimehr, Eur. Phys. J.: Spec. Top. **224**, 1469 (2015).
[5]D. Dudkowski, S. Jafari, T. Kapitaniak, N. V. Kuznetsov, G. A. Leonov, and A. Prasad, Phys. Rep. **637**, 1 (2016).
[6]M. Itoh and L. O. Chua, Int. J. Bifurcation Chaos **18**, 3183 (2008).
[7]F. Corinto, A. Ascoli, and M. Gilli, IEEE Trans. Circuits Syst. I **58**, 1323 (2011).
[8]J. C. Sprott, *Elegant Chaos: Algebraically Simple Chaotic Flows* (World Scientific Publishing, Singapore, 2010).
[9]L. Fortuna, M. Frasca, and M. G. Xibilia, *Chua's Circuit Implementations: Yesterday, Today and Tomorrow* (World Scientific Publishing, Singapore, 2009).
[10]A. Buscarino, L. Fortuna, M. Frasca, and G. Sciuto, *A Concise Guide to Chaotic Electronic Circuits* (Springer, Berlin DE, 2014).
[11]J. Piper, R. Jessica, and J. C. Sprott, IEEE Trans. Circuits Syst. II **57**, 730 (2010).
[12]L. O. Chua, Int. J. Electron. Commun. **46**, 250 (1992).
[13]K. Murali, M. Lakshmanan, and L. O. Chua, IEEE Trans. Circuits Syst. I **41**, 462 (1994).
[14]A. S. Elwakil and M. P. Kennedy, IEEE Trans. Circuits Syst. I **48**, 289 (2001).
[15]M. E. Yalçin, J. A. K. Suykens, and J. Vandewalle, *Cellular Neural Networks, Multi-Scroll Chaos and Synchronization* (World Scientific Publishing, Singapore, 2005).
[16]A. Buscarino, L. Fortuna, M. Frasca, and G. Sciuto, IEEE Trans. Circuits Syst. I **58**, 1888 (2011).
[17]C. Shen, S. Yu, J. Lu, and G. Chen, IEEE Trans. Circuits Syst. I **61**, 854 (2014).
[18]M. di Bernardo, F. Garofalo, L. Glielmo, and F. Vasca, IEEE Trans. Circuits Syst. I **45**, 133 (1998).
[19]M. Kennedy and L. O. Chua, IEEE Trans. Circuits Syst. **33**, 974 (1986).
[20]P. S. Linsay, Phys. Rev. Lett. **47**, 1349 (1981).
[21]T. Saito, IEEE Trans. Circuits Syst. **37**, 399 (1990).
[22]L. Fortuna, M. Frasca, S. Graziani, and S. Reddiconto, Nonlinear Dyn. **44**, 55 (2006).
[23]A. Buscarino, L. Fortuna, M. Frasca, and L. V. Gambuzza, Chaos **22**, 023136 (2012).
[24]M. P. Hanias and G. S. Tombras, Chaos, Solitons Fractals **40**, 246 (2009).
[25]E. Lindberg, K. Murali, and A. Tamasevicius, IEEE Trans. Circuits Syst. II **52**, 661 (2005).
[26]M. P. Kennedy, IEEE Trans. Circuits Syst. **41**, 771 (1994).
[27]P. Kvarda, Int. J. Bifurcation Chaos **12**, 2229 (2002).
[28]N. F. Rulkov and A. R. Volkovski, IEEE Trans. Circuits Syst. I **48**, 673 (2001).
[29]R. Modeste Nguimdo, R. Tchitnga, and P. Woafo, Chaos **23**, 043122 (2013).
[30]L. Minati, Chaos **24**, 033110 (2014).
[31]J. C. Sprott, Am. J. Phys. **68**, 758 (2000).
[32]L. Minati, in *Proceedings of the 8th International Symposium on Image and Signal Processing and Analysis, ISPA, Trieste, Italy* (2013), p. 748.
[33]L. Minati, Chaos **24**, 043108 (2014).
[34]L. Minati, Chaos **25**, 033107 (2015).
[35]P. Kvarda, Radioengineering **9**, 10 (2000).
[36]E. Lindberg, K. Murali, and A. Tamacevicius, in *Proceedings of the 14th International Workshop on Nonlinear Dynamics Electronic Systems, NDES2006, Dijon, France* (2006), p. 108.
[37]P. Mazumder and E. Rudnick, *Genetic Algorithms for VLSI Design, Layout and Test Automation* (Prentice Hall, Upper Saddle River, NJ, USA, 1998).
[38]"Evolvable systems: From biology to hardware," in *Second International Conference, Ices 98 Lausanne, Switzerland, September 23-25, 1998*, edited by M. Sipper (Springer, Berlin, DE, 2013).
[39]R. Hegger, H. Kantz, and T. Schreiber, Chaos **9**, 413 (1999).
[40]See http://ngspice.sourceforge.net for Software, documentation and credits.
[41]*Inductors for Decoupling Circuits, NLFV32-EF Type* (TDK Corporation, Tokyo, Japan, 2017).
[42]See http://www.lminati.it/listing/2017/a/ for experimental time-series.
[43]M. Ester, H. P. Kriegel, J. Sander, and X. Xu, "A density-based algorithm for discovering clusters in large spatial databases with noise," in *Proceedings of the Second International Conference on Knowledge Discovery and Data Mining (KDD-96)*, edited by E. Simoudis, J. Han, and U. M. Fayyad (AAAI Press, Cambridge, MA, USA, 1996).
[44]J. M. Grey and J. W. Gordon, J. Acoust. Soc. Am. **63**, 1493 (1978).
[45]J. D. Johnston, IEEE J. Sel. Areas Commun. **6**, 314 (1988).
[46]E. Ott, *Chaos in Dynamical Systems* (Cambridge University Press, Cambridge, UK, 2002).
[47]P. Oświęcimka, J. Kwapień, and S. Drożdż, Phys. Rev. E **74**, 016103 (2006).
[48]T. C. Halsey, M. H. Jensen, L. P. Kadanoff, I. Procaccia, and B. I. Shraiman, Phys. Rev. A **33**, 1141 (1986).
[49]J. W. Kantelhardt, S. A. Zschiegner, A. Bunde, S. Havlin, E. Koscielny-Bunde, and H. E. Stanley, Physica A **316**, 87 (2002).
[50]S. Drożdż, P. Oświęcimka, A. Kulig, J. Kwapień, K. Bazarnik, I. Grabska-Gradzińska, J. Rybicki, and M. Stanuszek, Inf. Sci. **331**, 32 (2016).
[51]H. E. Hurst, Trans. Am. Soc. Civ. Eng. **116**, 770 (1951).
[52]L. B. M. Silva, M. V. D. Vermelho, M. L. Lyra, and G. M. Viswanathan, Chaos, Solitons Fractals **41**, 2806 (2009).
[53]V. S. Anishchenko, V. Astakhov, A. Neiman, T. Vadivasova, and L. Schimansky-Geier, *Nonlinear Dynamics of Chaotic and Stochastic Systems: Tutorial and Modern Developments* (Springer, Berlin, Germany, 2007).
[54]S. T. Kingni, L. Keuninckx, P. Woafo, G. Van der Sande, and J. Danckaert, Nonlinear Dyn. **73**, 1111 (2013).
[55]L. Minati, Chaos **26**, 073103 (2016).
[56]J. M. Beggs and D. Plenz, J. Neurosci. **23**, 11167 (2003).
[57]J. T. Connor and R. D. Martin, IEEE Trans. Neural Networks **5**, 240 (1994).
[58]U. T. Eden and M. A. Kramer, J. Neurosci. Methods **190**, 149 (2010).
[59]E. V. Efremova and L. V. Kuzmin, in *Proceedings of the 1st IEEE International Conference on Circuits and Systems for Communications, 2002* (ICCSC '02), p. 300.
[60]J. H. B. Wijekoon and P. Dudek, Neural Networks **21**, 524 (2008).
[61]H. Torikai, T. Saito, and Y. Kawasaki, Int. J. Bifurcation Chaos **12**, 1207 (2002).
[62]T. Matsumoto, L. Chua, and K. Tokumasu, IEEE Trans. Circuits Syst. I **33**, 828 (1986).
[63]L. Keuninckx, G. Van der Sande, and J. Danckaert, IEEE Trans. Circuits Syst. II **62**, 891 (2015).
[64]S. Boccaletti, J. Kurths, G. Osipov, D. L. Valladares, and C. S. Zhou, Phys. Rep. **366**, 1 (2002).

[65] L. Faes, D. Kugiumtzis, A. Montalto, G. Nollo, and D. Marinazzo, Phys. Rev. E **91**, 032904 (2015).

[66] A. Kraskov, H. Stögbauer, and P. Grassberger, Phys. Rev. E **69**, 066138 (2004).

[67] I. Vlachos and D. Kugiumtzis, Phys. Rev. E **82**, 016207 (2010).

[68] T. Schreiber, Phys. Rev. Lett. **85**, 461 (2000).

[69] R. Vicente, M. Wibral, M. Lindner, and G. Pipa, J. Comput. Neurosci. **30**, 45 (2011).

[70] J. K. Hale, J. Dyn. Differ. Equations **9**, 1 (1997).

[71] N. F. Rulkov, M. M. Sushchik, L. S. Tsimring, and H. D. I. Abarbanel, Phys. Rev. E **51**, 980 (1995).

[72] H. D. I. Abarbanel, N. F. Rulkov, and M. M. Sushchik, Phys. Rev. E **53**, 4528 (1996).

[73] D. Chicharro and R. G. Andrzejak, Phys. Rev. E **80**, 026217 (2009).

[74] A. Kittel, J. Parisi, and K. Pyragas, Physica D **112**, 459 (1998).

[75] V. Rubezic, B. Lutovac, and R. Ostojic, "Linear generalized synchronization of two chaotic Colpitts oscillators," in *9th International Conference on Electronics, Circuits and Systems*, 2002, p. 223.

[76] B. S. Dmitriev, A. E. Hramov, A. A. Koronovskii, A. V. Starodubov, D. I. Trubetskov, and Y. D. Zharkov, Phys. Rev. Lett. **102**, 074101 (2009).

[77] R. Martínez-Guerra, J. L. Mata-Machuca, and A. Rodríguez-Martínez, "Generalized synchronization between Colpitts and Chua circuits," in *2013 IEEE 56th International Midwest Symposium on Circuits and Systems (MWSCAS), Columbus OH, USA*, 2013, p. 1423.

[78] D. Harte, *Multifractals* (Chapman & Hall, London, UK, 2001).

[79] D. Plenz, E. Niebur, and H. G. Schuster, *Criticality in Neural Systems* (Wiley, Hoboken, NJ, USA, 2014).

[80] J. G. Restrepo, E. Ott, and B. R. Hunt, Physica D **224**, 114 (2006).

[81] A. Arenas, A. Díaz-Guilera, J. Kurths, Y. Moreno, and C. S. Zhou, Phys. Rep. **469**, 93 (2008).